A Phase Locked Loop-based Approach to Real-time Modal Analysis on Synchrophasor Measurements

Kai Sun, *Member, IEEE*, Qiang Zhou, *Member, IEEE* and Yilu Liu, *Fellow, IEEE*

***Abstract*—This paper presents a Phase Locked Loop based approach for real-time estimation of electro-mechanical modal properties of slow-frequency oscillations in a power grid. The approach utilizes a close-loop feedback control system to automatically adjust a locally generated signal to optimally fit the targeted signal from real-time measurements in order to obtain modal properties directly from the local signal. The paper tests the approach on a variety of datasets including simulated and real synchrophasor data. Compared to a traditional spectral analysis based approach, this new approach has better adaptability and accuracy especially when the length of a measured signal is limited, or the signal contains modes with close frequencies or has floating modal properties, which is not unusual in a power grid due to its nonlinearity. Applied to wide-area synchrophasor measurements, the new approach may help system operators monitor slow-frequency oscillations, especially inter-area modes, which is important for a smart grid to maintain angular stability under disturbances.**

***Index Terms*—Inter-area mode; modal analysis; mode shape; Phase Locked Loop; phasor measurement unit; slow-frequency oscillation; spectral analysis; synchrophasor**

I. Introduction

DISTURBANCES in a power transmission system may cause slow-frequency oscillations in generators' rotor angles. If not damped effectively or under further disturbances, some oscillations may evolve into angular instability of the power system. A typical example is the August 1996 blackout event in the North America, in which the Western Interconnection experienced initial events, increasing vulnerability due to local protection actions, low-damped inter-area oscillations, and system islanding leading to cascading power outages. Therefore, online monitoring and understanding slow-frequency oscillations in the transmission system would be critical features of a smart grid.

In recent years, synchrophasors, e.g. Phasor Measurement Units (PMUs), are increasingly installed in power grids to provide GPS-synchronized measurements at a high sampling rate (typically, 30 samples per second). Those are ideal real-time data sources for detecting and monitoring low-frequency oscillations in power systems. If placed at dispersed critical locations, synchrophasors can provide continuous wide-area measurement data to an oscillation monitoring tool to estimate modal parameters in the data for a targeted oscillation mode. Those parameters include the oscillatory frequency, damping, phase and amplitude of the mode in the data from one synchrophasor and the coherency (i.e. correlation) between the data from different synchrophasors about that mode. Those parameters together indicate the shape of the mode.

Currently, spectral analysis-based oscillation monitoring methods are widely applied. A typical spectral analysis-based approach estimates the oscillatory frequency by fast Fourier transforms (FFT) on the data, apply the Prony analysis [1] or Wavelet transform [2] to estimate damping, and study the mode shape by cross-spectrum analysis [3]. However, the accuracy of such an approach is limited due to the nature of FFT algorithm: it has spectral leakage when fed with a finite-length of signal, and it only considers a finite number of discrete frequency components due to computational complexity. Thus, the estimated frequency and phase of a signal of interest are influenced heavily by nearby frequency components. Consequently, significant errors also exist in the other modal parameters. That disadvantage becomes obvious when several oscillation modes have close frequencies. Besides, in a power system, the signals captured by synchrophasors often show floating modal parameters, especially for frequencies and phases in transient periods following disturbances, which is due to the power system's nonlinear nature. Cross-spectrum analysis may have significant errors in mode shape estimation. For damping estimation, Prony analysis has errors in estimating damping in a signal with nonlinearity, and Wavelet transform decomposes a signal into multi-scales or multiple frequency bands, whose accuracy is limited by its scale resolution as well as the selection of basis wavelets.

This paper proposes a new real-time modal analysis approach based on the phase-locked loop (PLL) technique [4]-[8]. For a targeted oscillation mode, the new approach can estimate modal parameters more accurately and efficiently than a typical spectral analysis-based approach: first, it depends less on the number of discrete frequency components and the length of the measured signal because the floating frequency or phase of a signal about a targeted mode is adaptively tracked at a high

This work was supported by the Electric Power Research Institute (EPRI).

K. Sun and Y. Liu are with the University of Tennessee, Knoxville, TN 37996 (e-mail: kaisun@utk.edu and liu@utk.edu) and Q. Zhou is with Chrontel Inc., San Jose, CA 95131 (e-mail: qzhou99@gmail.com).

accuracy by a PLL; with accurate frequency and phase of the targeted mode, the other modal properties can be obtained only for an extracted signal about that mode without undesired interference from other nearby modes.

In the rest of the paper, Section II briefly introduces the PLL technique, Section III presents the proposed PLL-based approach, Section IV tests it by case studies, and finally, conclusions are drawn in Section V.

II. Phase Locked Loop Technique

A phase-locked loop (PLL) is a type of close-loop feedback control system that automatically adjusts specific modal properties, e.g. frequency and phase, of a signal rebuilt locally to lock on those of an input signal. Due to its feedback nature, the rebuilt signal can optimally fit the input signal. Thus, the frequency and phase can dynamically be estimated at a high accuracy. PLL has been successfully applied in several fields about power system signal analysis, e.g. fault detection and harmonic estimation [9]-[11].

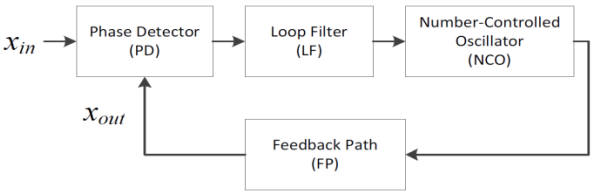

Fig. 1. PLL Algorithm

The structure of a discrete PLL is illustrated in Fig. 1, where x_{in} and x_{out} are input and rebuilt signals respectively with phases θ^{ref} and θ. Typically, the close loop contains four blocks: Phase Detector (PD), Loop Filter (LF), Number-Controlled Oscillator (NCO) and Feedback Path (FP). The PD compares two signals and produces an error signal proportional to their phase difference. The error signal goes through the LF (usually a low-pass filter) to drive an NCO to create an output phase θ going back through the FP. Despite the floating in the input signal, such a negative feedback loop makes the output phase θ be dynamically locked to the input phase θ^{ref}.

In a typical implementation of PLL, the PD may simply be a digital multiplier, the LF usually adopts a PI (proportional-integral) controller and the NCO is essentially an integrator converting frequency into phase. Fig. 2 illustrates a linearized Z-domain PLL model. $LF(z)$ and $NCO(z)$ are defined by (1) and (2), which will be adopted in this paper. In (1), K_P and K_I are respectively the gains of the proportional and integral paths influencing the tracking performance.

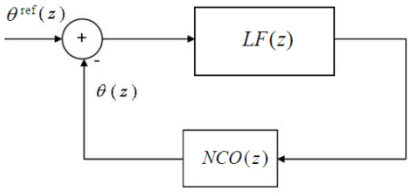

Fig. 2. PLL Algorithm in Z-Domain

$$LF(z) = K_P + \frac{K_I z^{-1}}{1 - z^{-1}} \tag{1}$$

$$NCO(z) = \frac{z^{-1}}{1 - z^{-1}} \tag{2}$$

III. Proposed Approach

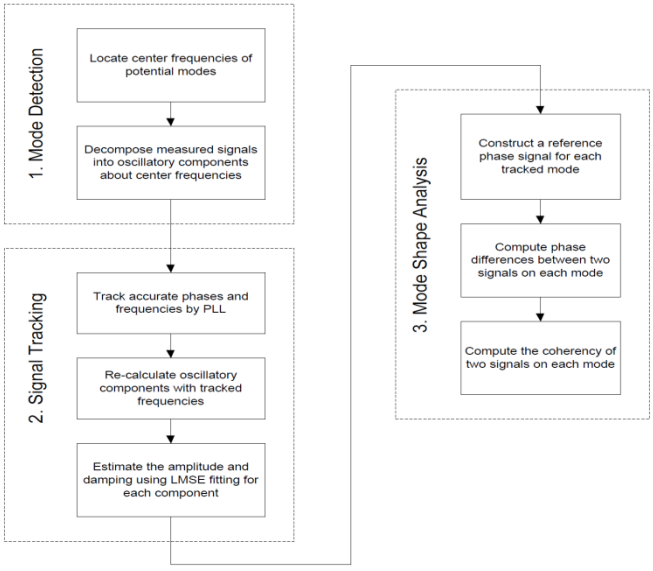

Fig. 3. Proposed PLL-based approach

The proposed PLL-based approach takes three steps as shown in Fig. 3: 1) mode detection, 2) signal tracking, 3) mode shape analysis. Assume that N dispersed synchrophasors in a power grid are used to monitor slow-frequency oscillations. Their synchronized measurements over a time window are represented by N time-series signals $x_1(1)$~$x_1(L)$, …, $x_N(1)$~$x_N(L)$ at the interval of Δt (1/30 seconds for PMU measurements). $T \triangleq L \times \Delta t$ is the length of the time window. Detailed tasks of the three steps are presented below.

A. Mode Detection

This step is to identify low-frequency oscillations in each signal x_i measured by a synchrophasor. According to knowledge on the power system, a number (denoted by M) of targeted oscillation modes can be preselected with initial estimates on frequencies, denoted by f^0_1~f^0_M, and expected standard deviations, denoted by σ^0_1~σ^0_M. As defined in equation (3), M complex Gaussian filters are adopted to decompose x_i in the frequency domain into M oscillatory components s_{im} (i=1~N, m=1~M), each with respect to one single center frequency, i.e. f^0_m.

$$g_m(f) = \frac{\exp\left[-\frac{(f - f_m^0)^2}{2(\sigma_m^0)^2}\right]}{\sqrt{2\pi}\sigma_m^0} \quad m = 1 \sim M \tag{3}$$

s_{im} is calculated by the linear convolution operation:

$$s_{im} = x_i \otimes g_m \tag{4}$$

B. Signal Tracking

For each component s_{im} in signal x_i, PLL is used to accurately track its phase, named θ_{im}. Selection of K_P and K_I should consider the power of s_{im} and can be optimized the fastest

tracking. The proposed PLL-based approach selects K_P and K_I as follows to meet the requirement of real-time application.

i) Select typical data on x_i over a time window and estimate the power (denoted by A_{im}) of s_{im} by the corresponding peak in the FFT plot on the data.
ii) Let $K_{P0}=1/A_{im}$ and $K_{I0}=0.01K_{P0}$ as initial values of K_P and K_I. Then, test the tracking performances of the PLL with sample values of K_P and K_I in $0.1K_{P0}$~$10K_{P0}$ and $0.1K_{I0}$~$10K_{I0}$ and select the best K_P and K_I.

With θ_{im} tracked, the instantaneous frequency f_{im} for component s_{im} in signal x_i can be estimated by

$$f_{im}=\frac{d\theta_{im}}{dt} \quad i=1\sim N \tag{5}$$

The above mode detection and PLL-based signal tracking can also be executed on signal x_i over a time window by the following iterative procedure for more accurate modal estimation, especially if x_i has modes with close frequencies:

i) For a targeted mode m, select f^0_m (based on, e.g., FFT of the data), σ^0_m, a small positive number Δ for convergence checking, and $\lambda\in(0, 1)$ for iteration speed control.
ii) Calculate component s_{im} by (3) and (4) and perform the PLL algorithm to track the frequency as f_{im}.
iii) If $|f_{im}-f^0_m|/f^0_m<\Delta$, exit; otherwise, let f_{im} and $\lambda\sigma^0_m$ be the new f^0_m and σ^0_m, and go back to step ii).

It should be noted that for a signal containing two modes with very close frequencies, its FFT plot may just indicate one peak if the time window is not long enough. In step i) of the above iterative procedure, their initial frequencies may be selected at two sides near that peak to avoid converging to the same mode.

After the estimated frequencies about mode m are obtained from all N signals, i.e. f_{1m}~f_{Nm}, use their mean value, denoted by f_m, as the final estimate of the frequency. Then, similar to (4), apply a complex Gaussian filter at f_m with a reduced deviation σ_m, e.g. $\sigma^0_m/5$, to signal x_i to obtain y_{im} as a better approximation of the m-th oscillatory component. There is

$$x_i \approx \sum_{m=1\sim M} y_{im} \tag{6}$$

The next step is obtain damping coefficient d_{im} and amplitude a_{im} of component y_{im} together by minimizing either of the following objective functions

$$c_1(a_{im},d_{im})=\sum_{l=1}^{L}\left|\left|y_{im}(l\cdot\Delta t)\right|-a_{im}e^{-d_{im}\cdot l\cdot\Delta t}\right|^2 \tag{7a}$$

$$c_2(a_{im},d_{im})=\sum_{k=1}^{L}\left|\ln\left|y_{im}(l\cdot\Delta t)\right|-[\ln(a_{im})-d_{im}\cdot l\cdot\Delta t]\right|^2 \tag{7b}$$

For instance, the second one is solved as a LMSE (Least Mean Square Error) linear fitting problem.

C. Mode Shape analysis

For a specific center frequency f_m, construct a reference phase signal at each of L time steps of Δt

$$u(f_m,l)=e^{-j2\pi f_m\cdot l\cdot\Delta t}, l=1\cdots L \tag{8}$$

Calculate

$$q_{im}(f_m)=\frac{1}{L}\sum_{l=1}^{L}y_{im}(l\cdot\Delta t)\cdot u(f_m,l) \tag{9}$$

$q_{1m}(f_m)$~$q_{Nm}(f_m)$ together determine the mode shape of the oscillation mode at f_m:

- Magnitude $|q_{im}(f_m)|$ measures the average power of y_{im}'s component at f_m, which, in fact, indicates the participation factor of x_i in oscillation at that frequency.
- $q_{im}(f_m)$'s phase angle (denoted by $\hat{\theta}_{im}$) represents the phase of component y_{im} at f_m over the time window. Thus, $\hat{\theta}_{im}-\hat{\theta}_{jm}$ (i and j=1~N) gives the phase difference between two signals x_i and x_j at f_m.

Each of the M modes could be either a local mode or an inter-area mode. A squared linear coherency index employed in [3] can be calculated for any two components y_{im} and y_{jm} (i and j=1~N) from apart locations. If the coherency index is high (e.g. >0.5), the mode at f_m can be regarded as an inter-area mode over a region covering synchrophasors i and j. However, since that index is calculated based on cross-spectrum estimation, its accuracy is influenced by the problems mentioned in Section I. The proposed PLL-based approach is able to directly estimate coherency between two signals from their average powers at a specific frequency. As defined in (10), a new coherency index $r_{ij}\in[0, 1]$ is calculated for signals x_i and x_j at f_m over the latest T:

$$r_{ij}(f_m)=\frac{|q_{im}(f_m)|\cdot|q_{jm}(f_m)|}{|q_{im}(0)|\cdot|q_{jm}(0)|} \tag{10}$$

where $|q_{im}(0)|$ and $|q_{jm}(0)|$ equal the average powers of y_i and y_j at f_m over the time window, e.g.

$$q_{im}(0)=\frac{1}{L}\sum_{n=1}^{L}y_{im}(n) \tag{11}$$

If $r_{ij}(f_m)$ is small (e.g. <0.5) for any pair of i and j, the mode at f_m can be regarded as a local mode.

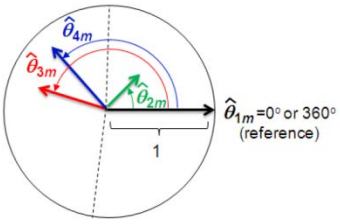

Fig. 4. "Phase clock" on the mode shape at f_m

The proposed PLL-based approach can accurately estimate modal parameters for both local and inter-area modes. System operators in control rooms usually pay more attention to inter-area modes. For an inter-area mode m, $\hat{\theta}_{im}-\hat{\theta}_{jm}$ (i and j=1~N) gives the phase difference between two signals x_i and x_j at f_m. Thus, for any pair of signals, the phase difference and the coherency index can be calculated at a specific frequency. All such phase differences and coherency indices together present the mode shape of the oscillation mode at the frequency. As illustrated in Fig. 4, let $\hat{\theta}_{1m}$=0° and 360° (the phase reference) and draw N phasors $r_{1j}(f_m)\angle\hat{\theta}_{jm}$ in a unit circle as a "phase clock" on the mode shape at f_m. The length of each pointer indicates how coherent the corresponding signal is with signal x_1. The N phasors can be divided into a number of clusters by their phase differences. The clustering of N phasors may

indicate a potential out-of-step pattern of generators [12][13]. For example, the biggest two phase differences between any adjacent phasors in Fig. 4 are $|\hat{\theta}_{4m} - \hat{\theta}_{2m}|$ and $|360^o - \hat{\theta}_{3m}|$, which indicate 2 clusters {1, 2} and {3, 4}.

IV. Case Studies

Three groups of case studies on the proposed PLL-based approach are conducted respectively using generated signals, data from simulation and historical event data.

A. Generated signals

To compare with the spectral analysis based approach in terms of accuracies of phase and coherency estimation, the proposed approach is first tested using two designated cosine signals in the form of

$$x_i = A_{i1}\cos(2\pi f_1 t + \theta_{1i}) + A_{i2}\cos(2\pi f_2 t + \theta_{i2}) + s_{i0} \stackrel{\text{def}}{=} s_{i1} + s_{i2} + s_{i0} \qquad i = 1 \text{ or } 2 \qquad (12)$$

where s_{i1} and s_{i2} (i=1 or 2) are oscillatory components about two targeted modes at frequencies f_1 and f_2, respectively, and s_{i0} represent noise or a background signal containing the modes of less interest. The goal is to estimate the phase difference and coherency between x_1 and x_2 for each targeted mode.

Let f_1=0.25Hz and f_2=1.05Hz, which are in the range of typical oscillatory frequencies in power systems. Assume Δt=1/30 seconds and the following parameters for two signals: A_{11}=2, A_{12}=1, θ_{11}=60°, θ_{12}=-45°, A_{21}=2.5, A_{22}=0.5, θ_{21}=θ_{22}=0°. Obviously, the phase differences on the 0.25Hz model and 1.05Hz mode are 60° and -45°, respectively. Consider T=10s, 20s and 40s (i.e. 2.5, 5 and 10 periods of the slower 0.25Hz mode) to study how the time window of signals influences estimation accuracy. Let s_{20}=0 and s_{10}= 0.5·cos(2π·0.6t), which indicates a 0.6Hz local mode only existing in x_1. Set initial estimates of f_1 and f_2 at 0.2Hz and 1.0Hz with 0.05Hz error, and in the PLL algorithm, set σ^0_1=σ^0_2=0.25, K_P=0.2 and K_I=0.002. Since the frequencies of two modes are not very close, the iterative procedure is unnecessary.

For comparison, the following Power Spectral Density (PSD) based approach is also tested on x_1 and x_2:

i) Estimate the frequencies of two targeted modes from peaks in the FFT plot on x_1-x_2 over T
ii) Estimate the coherencies and phase differences about x_1 and x_2 over T at the two estimated frequencies: estimate the magnitude squared coherence defined in [3] by their PSDs and cross PSD using the Welch's averaged periodogram method [14], and estimate the phase difference by the angle of their cross PSD.

For different lengths of T, Table I gives estimated frequencies and phase differences by using the PLL-based approach (the first row in bold font) without the iterative procedure versus the PSD-based approach (the second row). Percentage errors are given in parentheses. Table I also gives the estimated frequencies on the 0.6Hz local mode by two approaches. The PLL algorithm uses 0.5Hz (i.e. 0.1Hz error) as the initial frequency and is applied to x_1-x_2 to give the estimates.

From the table, the PLL-based approach has much higher accuracy in estimating phase differences for T=10s, 20s or 40s. When T=20s or 40s, it also surpasses the PSD-based approach in estimating frequencies. For illustration, Fig. 5 shows the PLL tracking results on x_1-x_2, s_{11}-s_{21} (0.25Hz mode) and s_{12}-s_{22} (1.05Hz mode) for T=10s and 20s. From the figure, when T is only 10s, the phase differences are accurately estimated (only 0.5% error from Table I). When T increases, signals are tracked better to give more accurate estimates for both frequencies and phase differences.

Regarding coherency estimation for two targeted modes, Fig. 6 compares two approaches with different lengths of T. More reasonably, the PLL-based approach shows two spikes corresponding to the 0.25Hz and 1.05Hz modes and estimates the coherency to be low at the other frequencies.

TABLE I
ESTIMATED FREQUENCIES AND PHASE DIFFERENCES AND THEIR ERRORS BY THE PLL-BASED (1ST ROW) AND PSD -BASED (2ND ROW) APPROACHES

Estimated parameters		T=10s	T=20s	T=40s
0.25Hz Mode	Freq. (Hz)	**0.214 (14.4%)**	**0.246 (1.6%)**	**0.250 (0.0%)**
		0.234 (6.4%)	0.234 (6.4%)	0.264 (5.6%)
	Phase Diff.(deg.)	**59.725 (0.5%)**	**59.992(0.0%)**	**60.000(0.0%)**
		55.054 (8.2%)	59.991(0.0%)	60.066(0.1%)
1.05Hz Mode	Freq. (Hz)	**1.057 (0.7%)**	**1.048 (0.2%)**	**1.050 (0.0%)**
		1.055 (0.5%)	1.055 (0.5%)	1.055 (0.5%)
	Phase Diff.(deg.)	**-45.207(0.5%)**	**-45.001(0.0%)**	**-45.000 (0.0%)**
		-44.083 (2.0%)	-44.436(1.3%)	-45.011(0.0%)
0.6Hz Mode	Freq. (Hz)	**0.617 (2.8%)**	**0.593 (1.2%)**	**0.600 (0.0%)**
		0.586 (2.3%)	0.586 (2.3%)	0.586 (2.3%)

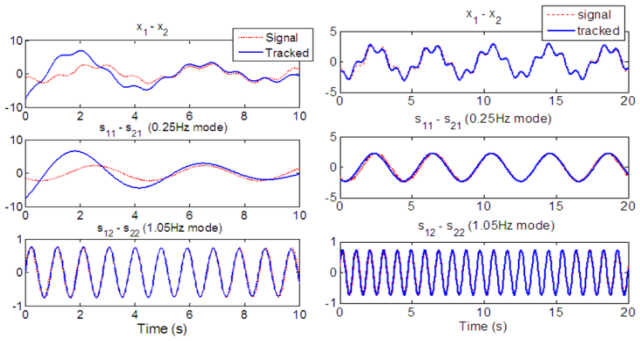

(a) T=10s (b) T=20s

Fig. 5. Results from the PLL-based approach

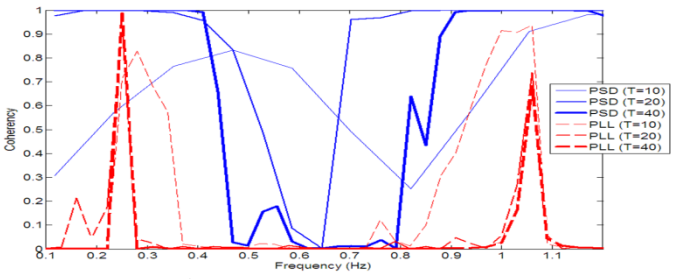

Fig. 6. Comparison of coherency estimation

In the next test, let s_{10}=s_{20}=0.5·cos(2π·0.6t)+0.02·t+1.5, which combines a 0.6Hz component, a dc component and a linear component. The estimation results are compared in Table II for two approaches. The PLL-based approach more accurately estimate phase differences. The 0.6Hz mode is

already eliminated by the subtraction operation x_1-x_2, but it can be detected from either x_1 or x_2. Its frequency estimates by two approaches are also given in the table. The PLL-based approach uses 0.5Hz as an approximate initial estimate for the mode and is applied to data of x_1. Fig. 7 compares the coherencies estimated by two approaches. The PLL-based approach indicates three peaks at the two targeted mode and the 0.6Hz mode in the background signal.

TABLE II
ESTIMATED FREQUENCIES AND PHASE DIFFERENCES AND THE ERRORS BY THE PLL-BASED (IN BOLD) AND SPECTRAL ANALYSIS-BASED APPROACHES

Estimated parameters		T=10s	T=20s	T=40s
0.25Hz Mode	Freq. (Hz)	**0.214 (14.4%)**	**0.246 (1.6%)**	**0.250 (0.0%)**
		0.234 (6.4%)	0.234 (6.4%)	0.264 (5.6%)
	Phase Diff.(deg.)	**59.723 (0.5%)**	**59.921 (0.1%)**	**60.001 (0.0%)**
		21.316(64.5%)	44.810(25.3%)	59.996(0.0%)
1.05Hz Mode	Freq. (Hz)	**1.057 (0.7%)**	**1.048 (0.2%)**	**1.050 (0.0%)**
		1.055 (0.5%)	1.055 (0.5%)	1.055 (0.5%)
	Phase Diff.(deg.)	**-45.350(0.5%)**	**-44.998(0.0%)**	**-45.000(0.0%)**
		-40.959(9.0%)	-44.254(6.1%)	-45.010(0.0%)
0.6Hz Mode	Freq. (Hz)	**0.611 (1.8%)**	**0.598 (0.3%)**	**0.595 (0.8%)**
		0.586 (2.3%)	0.586 (2.3%)	0.615 (2.5%)

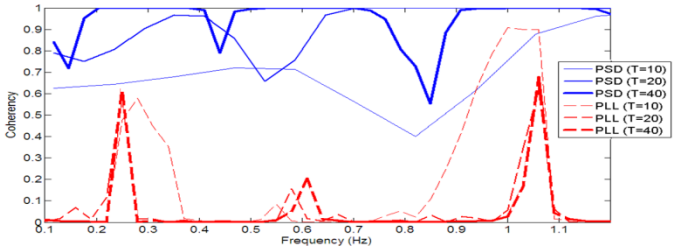

Fig. 7. Comparison of coherency estimation

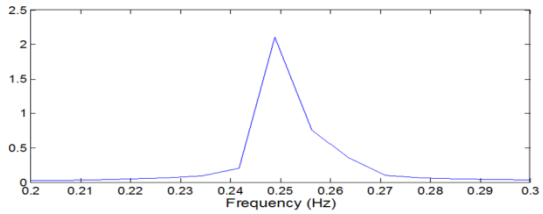

Fig. 8. FFT of x_1-x_2 over a 200s time window

To test the performance of the PLL-based approach on signals containing modes with very close frequencies, f_2 in the above signals x_1 and x_2 is changed to 0.26Hz, i.e. only 0.01Hz higher than f_1. Also, let s_{10} and s_{20} be Gaussian noises added to two signals, with a signal-to-noise ratio equal to 20dB. Due to the very small frequency difference, the time window is extended to 200s and 300s. Note that for T=200s, FFTs of the signals cannot tell two frequencies. As indicated by Fig. 8, the FFT plot of x_1-x_2 only shows one peak at 0.249Hz.

The iterative procedure of the PLL-based approach is applied in this case. Set initial estimates of f_1 and f_2 at 0.24Hz< f_1 and 0.27Hz>f_2 with 0.01Hz errors. Let $\sigma^0_1=\sigma^0_2=0.005$ and $\lambda=0.7$ and allow 5 times of iterations. Table III gives the results of the PLL-based approach (numbers in bold) and the PSD-based approach. The values before and after the arrow are respectively the results from the 1st and the 5th iterations. The PSD-based approach fails in differentiating the two modes for T=200s. For T=300s, it cannot correctly estimate the phase difference for the 0.26Hz mode. The PLL-based approach still works for T=200s, and it has much better overall performance than the PSD-based approach.

TABLE III
ESTIMATED FREQUENCIES AND PHASE DIFFERENCES AND THE ERRORS BY THE PLL-BASED (IN BOLD) AND SPECTRAL ANALYSIS-BASED APPROACHES

Estimated parameters		T=200s	T=300s
0.25Hz Mode	Freq. (Hz)	**0.247 (1.2%) → 0.249 (0.4%)**	**0.253 (1.2%) → 0.249 (0.4%)**
		0.249 (0.4%)	0.249 (0.4%)
	Phase Diff.(deg.)	**60.64 (1.1%) → 60.71 (1.2%)**	**60.20 (0.3%) → 60.28 (0.5%)**
		57.97 (3.4%)	59.83 (0.3%)
0.26Hz Mode	Freq. (Hz)	**0.267 (2.7%) → 0.264 (1.5%)**	**0.257 (1.2%) → 0.260 (0.0%)**
		0.249 (4.2%)	0.260 (0.0%)
	Phase Diff.(deg.)	**-41.18 (8.5%) → -46.80 (4.0%)**	**-41.03 (8.8%) → -45.54(1.2%)**
		57.97(228.9%)	52.99 (217.8%)

B. *179-bus test system*

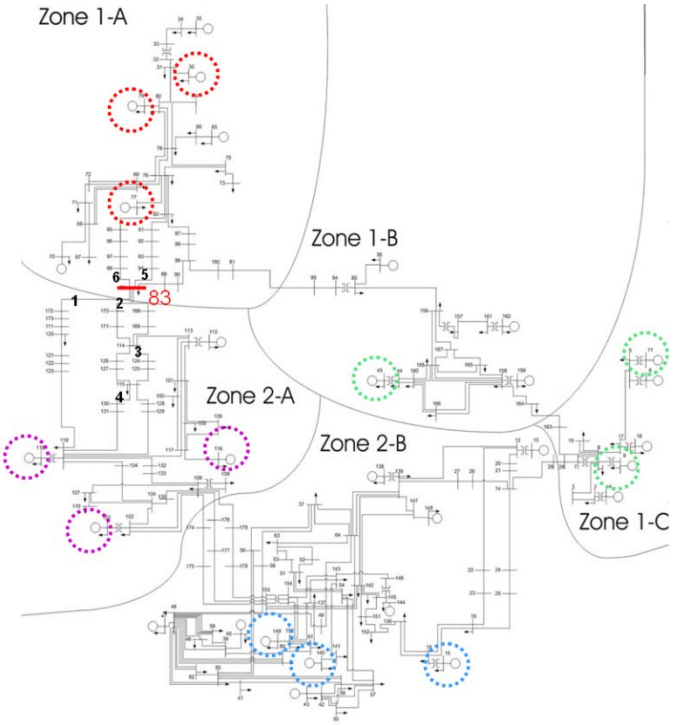

Fig. 9. 179-bus power system

The PLL-based approach is also tested on a 179-bus power system having 29 generators, 179 buses and 263 branches in 5 zones, as shown in Fig. 9. The system is a simplified model of the Western Interconnection ac system in North America. The power-flow base case has totally 60.8GW load. A generation coherency study by EPRI's DYNRED software identifies four generation clusters as indicated in Table IV. Assume that each cluster is monitored by a group of synchrophasors placed at three big generators (underlined in Table IV). Thus, the average angles θ_1~θ_4 of four synchrophasor groups be monitored for oscillations between generation clusters.

Consider six sequential three-phase faults at 40s intervals starting from t=0s on lines 83#-172, 83#-170, 114#-124, 115#-130, 83#-94 and 83#-98, where "#" indicates the fault bus. Each fault lasts 6 cycles followed by tripping the fault line. Fault locations are indicated by numbers 1~6 in Fig. 9. Those contingencies are close to the interface at bus 83, which corresponds to the California-Oregon Intertie involved in the western blackout in August 1996. Simulate that sequence of contingencies by TSAT of Powertech Labs. Fig. 10 gives rotor angles of all generators. The 12 generators monitored by synchrophasors are highlighted. From the figure, slow-frequency oscillations appear following each contingency. Their amplitudes increase until generators lose synchronism after the 6th contingency. The simulation results on θ_1~θ_4 are regarded as synchrophasor data in the test below.

TABLE IV
GENERATOR CLUSTERING

Clusters	Generator buses and PMU locations	Territory
1	30, 35, 65, 70, 77, 79	Zone 1-A
2	103, 112, 116, 118	Zone 2-A
3	13, 15, 40, 43, 47, 138, 140, 144, 148, 149	Zone 2-B
4	4, 6, 9, 11, 18, 36, 45, 159, 162	Zones 1-B and C

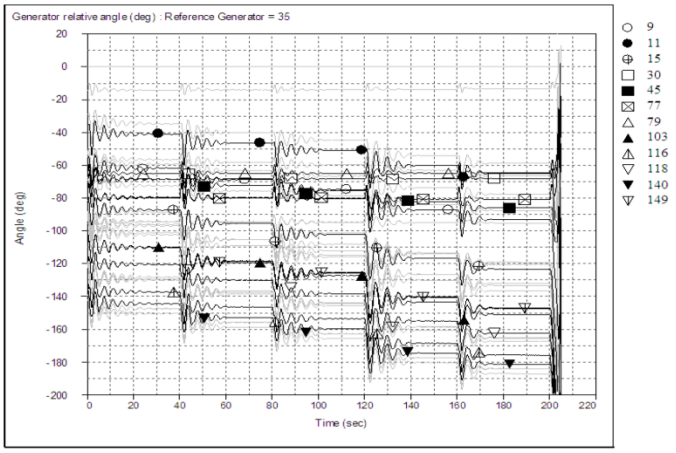

Fig. 10. Angles of generators (angles from 12 synchrophasors are highlighted)

Every 0.1s, conduct modal analysis on the latest 40s (i.e. T) synchrophasor data. Fig. 11 gives the FFT plots on θ_1-θ_2, θ_1-θ_3 and θ_1-θ_4 over time windows 120-160s and 160-200s. Two peaks indicate two oscillation modes at about 0.2Hz and 1.05Hz. The first one is the dominant mode, which is tracked below as an example. Set its standard deviation σ_1^0=0.1, K_P=0.2, K_I=0.002, and the initial estimate of the frequency at 0.2Hz. The iterative procedure with the PLL-based approach is not needed for this case since that mode is apart from the other one. Regarding that mode, Fig. 12 gives the modal analysis results from the PLL-based approach. From Fig. 12(a), its frequency floats between 0.17 and 0.29Hz. Fig. 12(b) and (c) gives the phase differences and the absolute phase differences between cluster 1 and the others, which indicate that cluster 1 oscillates against the other three following each contingency. That indicates a critical interface, i.e. 1-234, where angle separation may develop. Fig. 12(d) confirms that the mode is not a local mode. Fig.12(e) gives the damping coefficient estimated by the PLL-based approach.

Then, interface 1-234 is compared to another interface 14-23, which basically match the Western separation scheme. For two interfaces, Fig. 13 gives the plots on the angle differences and the absolute phase differences estimated by the PLL-based approach. Two angle differences are respectively equal to θ_1-($\theta_2^+\theta_3^+\theta_4$)/3 and ($\theta_1$+$\theta_4$)/2-($\theta_2^+\theta_3$)/2. Interface 14-23 has a bigger angle difference but a smaller phase difference.

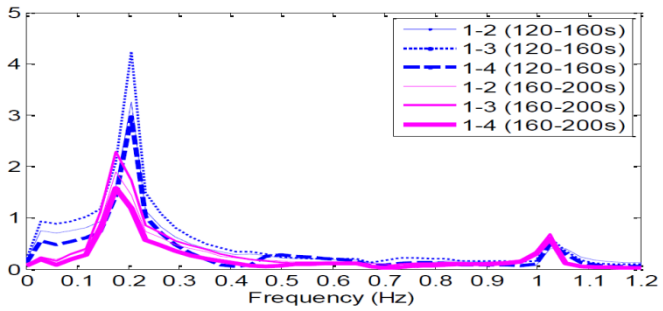

Fig. 11. FFT results over 120-160s and 160-200s

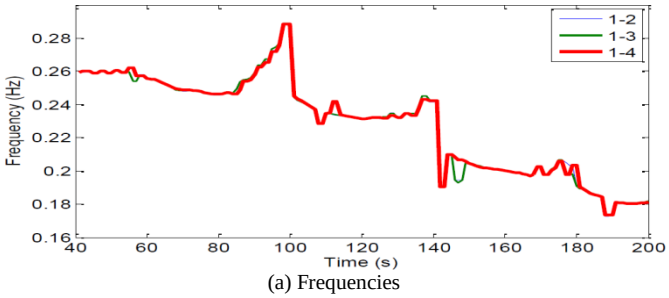

(a) Frequencies

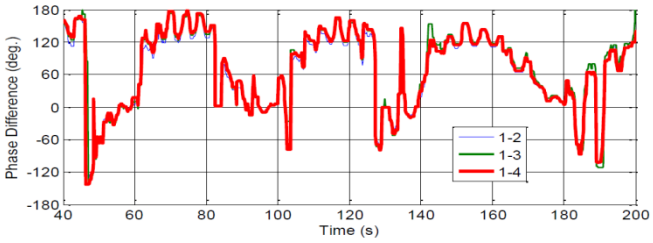

(b) Phase differences

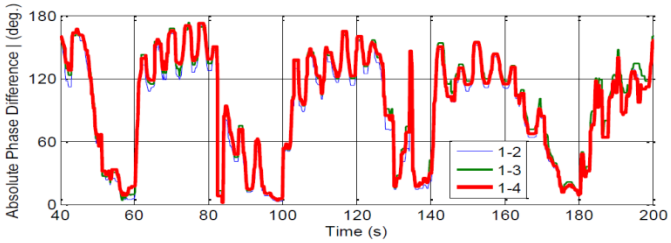

(c) Absolute Phase differences

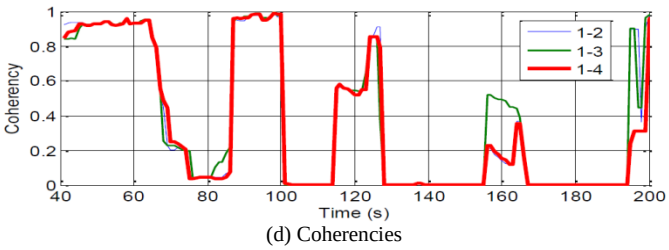

(d) Coherencies

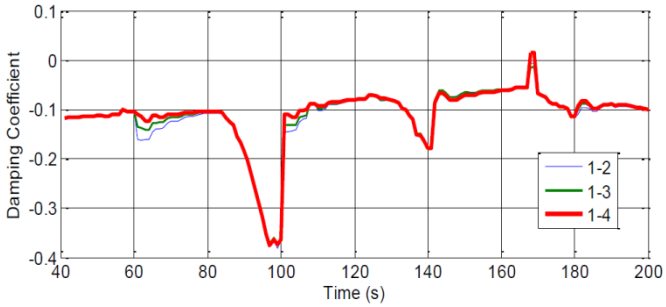

(e) Damping coefficients

Fig. 12. Estimation results on cluster pairs 1-2, 1-3 and 1-4 for the 0.2Hz mode

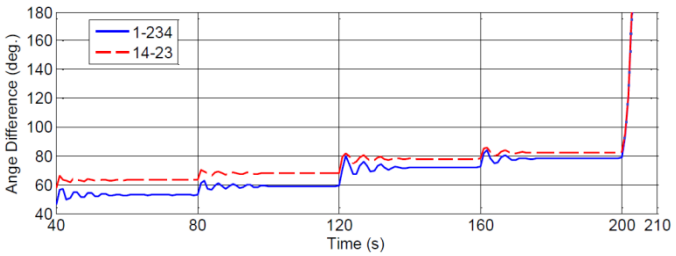

(a) Angle distances

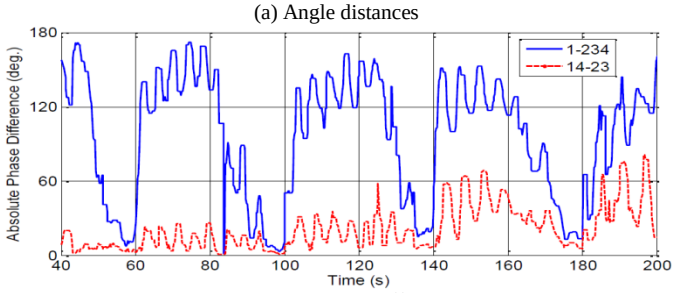

(b) Absolute Phase differences

Fig. 13. Estimation results on two interfaces about the 0.2Hz mode

C. *FNET data*

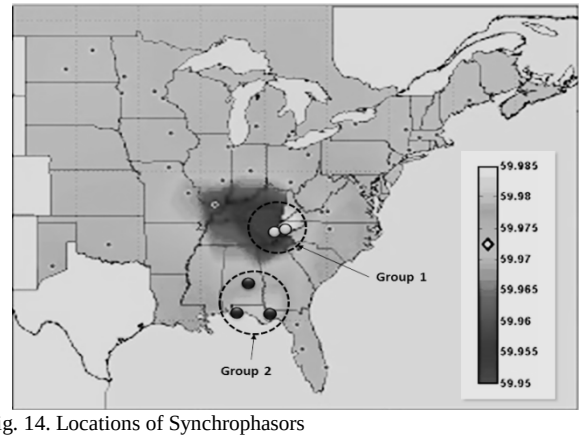

Fig. 14. Locations of Synchrophasors

The event data are from FNET[15], i.e. a wide-area frequency measurement network based on distribution-level synchro-phasors, called Frequency Disturbance Recorders (FDRs), providing synchronized measurements at 10 samples per second. In April 25-28, 2011, a tornado outbreak caused severely impacts on power transmission systems in the south-east US. One oscillation event in TVA system captured by FNET is used to test the proposed PLL-based approach. During the event, part of TVA system oscillated against neighboring systems. Data from 5 FDRs are utilized: two in the Tennessee, one in Alabama and two in Florida, as shown in Fig. 14. Frequency oscillations starting from 21:22:18 UTC captured by the 5 FDRs are shown in Fig. 15, indicating two groups: the two FDRs in Tennessee oscillated against the other three at almost opposite phases.

Fig. 16 gives FFT plots on the measured frequencies over the first 30s time window, and indicates two oscillation modes at around 0.59Hz and 0.66Hz. Set standard deviation $\sigma_1^0=\sigma_2^0=0.05$, $K_P=20$ and $K_I=0.2$. Let 0.55Hz and 0.7Hz be initial guesses of two oscillatory frequencies. Respectively consider T=13s and 26s, i.e. about 8 and 16 times of the periods of the two modes. The PLL-based approach is applied to the difference between the average frequencies of the two FDR groups to estimate the two oscillatory frequencies. Then the real-time phase difference between the two groups is estimated and compared with the result from the PSD-based approach. In this case, the iterative procedure with the PLL-based approach is not applied.

From Fig. 17(a), the time window of 13s is insufficient to differentiate the two oscillation modes from FFT since the oscillatory frequencies are 0.07Hz apart. Therefore, the PSD-based approach fails to estimate the phase difference, as shown in Fig. 17(b). The PLL-based approach successfully tracks the data based on the initial guesses on two oscillatory frequencies, as shown in Fig. 17(c). The estimated frequencies are given in Fig. 17(d). The approach estimates the phase differences between two FDR groups to be around -120° and -160° for two oscillation modes. From Fig. 18(a), the time window of 26s is sufficient to tell two oscillation modes from FFT. However, the PSD-based approach does not perform well in estimating the phase differences about two modes, as shown in Fig. 18(b). From Fig. 18(c)-(e), the PLL-based approach tracks the data and more accurately estimates the oscillatory frequencies and phase differences.

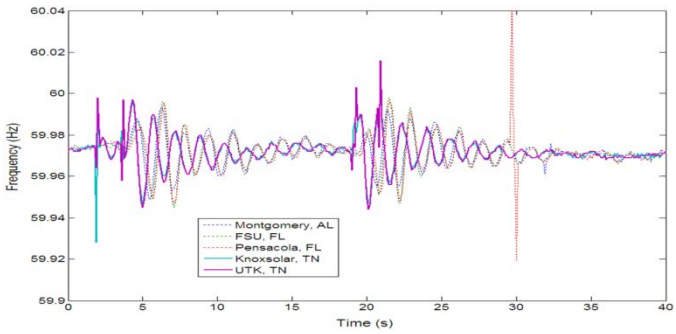

Fig. 15. Frequency oscillations (Baseline time: 21:22:18 UTC on 4/27/2011)

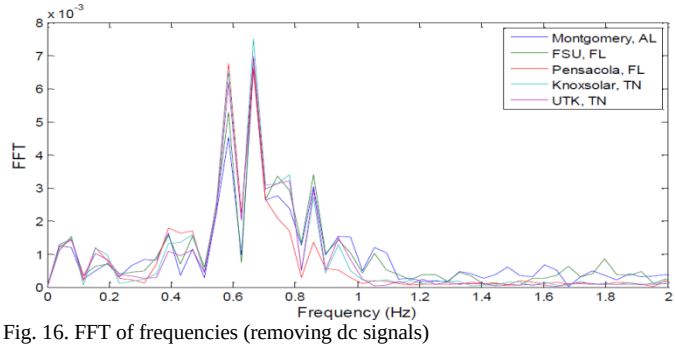

Fig. 16. FFT of frequencies (removing dc signals)

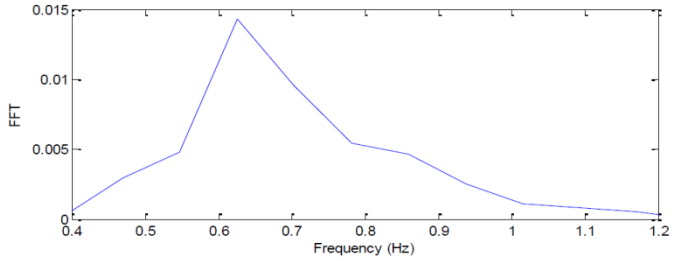

(a) FFT of the frequency difference

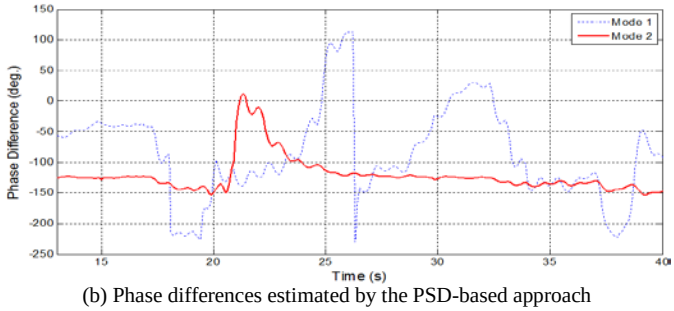

(b) Phase differences estimated by the PSD-based approach

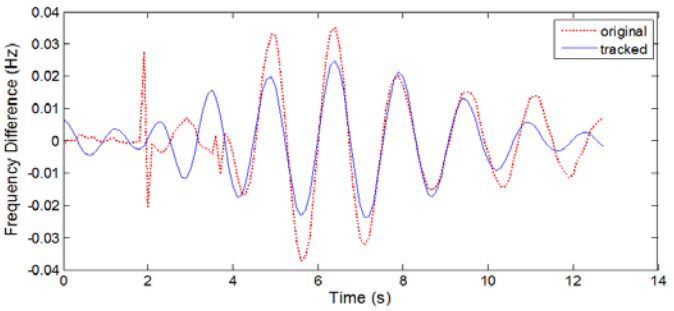

(c) Actual and tracked frequency difference

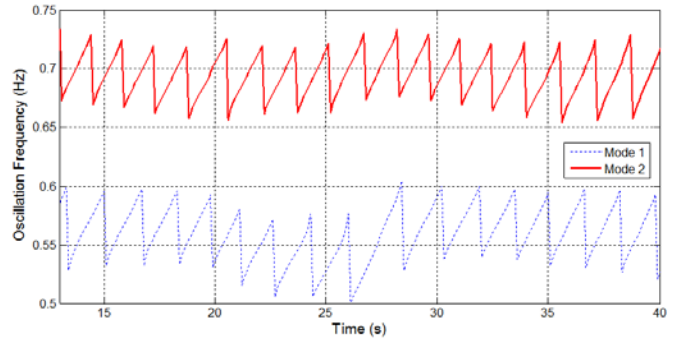

(d) Oscillatory frequencies estimated by the PLL-based approach

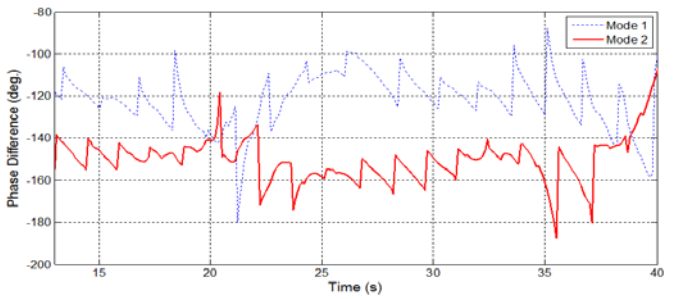

(e) Phase differences estimated by the PLL-based approach

Fig. 17. Results with T=13s

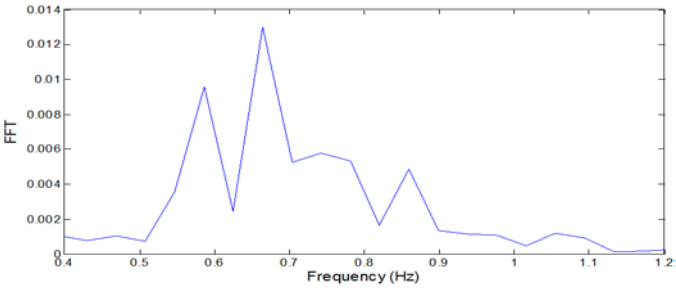

(a) FFT of the frequency difference

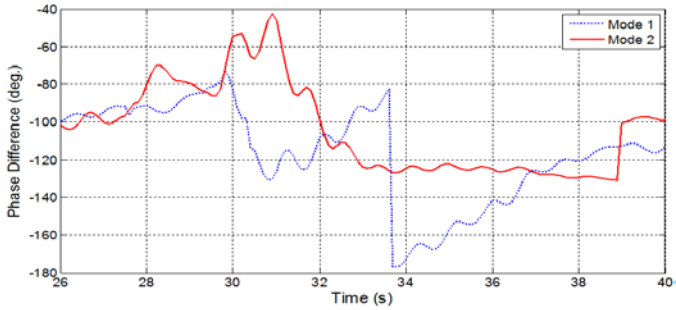

(b) Phase differences estimated by the PSD-based approach

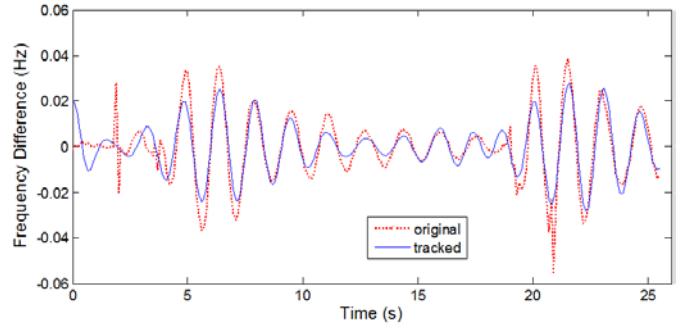

(c) Actual and tracked frequency difference

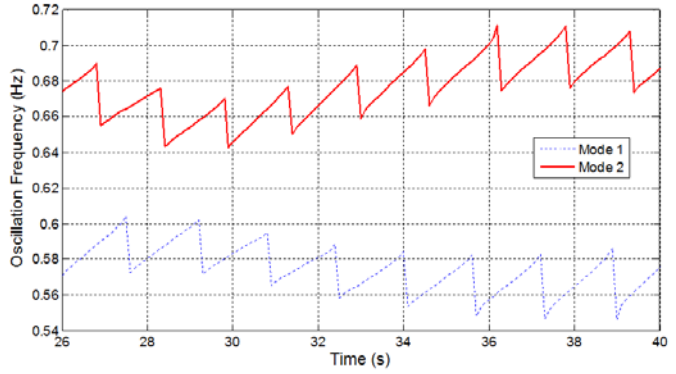

(d) Oscillatory frequencies estimated by the PLL-based approach

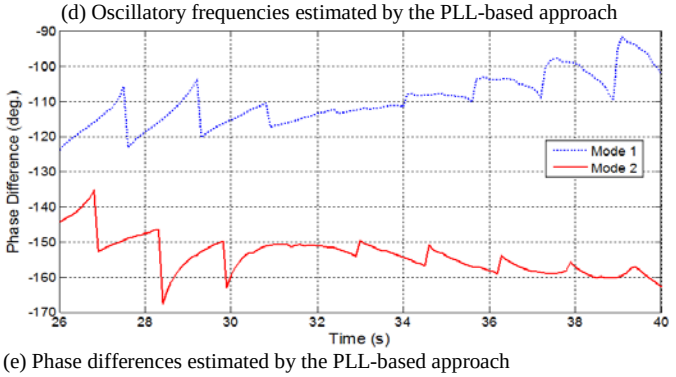

(e) Phase differences estimated by the PLL-based approach

Fig. 18. Results with T=26s

For this case, the PLL-based approach takes 13 seconds to accurately track the target modes because PLL is initialized at t=0s (immediately after the event is detected) and needs to collect data over a sufficient time window that is inversely proportional to the frequency of the targeted mode. Once PLL tracks the targeted mode in continuously measured data, if the real-time frequency of the mode does not significantly change, the close-loop feedback control nature with PLL enables accurately following that mode. That is an important feature for real-time power system monitoring. The time spent by a single run of the PLL-based approach over 40s data is less than 0.03s in MATLAB on a 3.4GHz CPU computer.

It can be noticed that there are ripples in the oscillatory frequencies and phase differences estimated by the PLL-based approach. The sizes of those ripples are related to the errors of the initial guesses on the frequencies and other PLL parameters. The ripples can be reduced when the iterative procedure mentioned above is applied to data over each time window.

V. Conclusion

This paper has proposed a new PLL-based approach for real-time estimating electro-mechanical modal properties of oscillations in a power system. The new approach is compared to a typical PSD-based approach by detailed case studies on generated signals, simulated synchrophasor data, and real synchrophasor data. Case studies indicate that this new approach has better adaptability and accuracy especially when the targeted signal has modes with close frequencies or floating modal properties, or has a limited length of data available.

VI. References

[1] J.F. Hauer, et al, "Initial Results in Prony Analysis of Power System Response Signals", IEEE Trans. Power Syst., vol. 5, No. 1, pp. 80-89, Feb 1990

[2] K. Hur, S. Santoso, "Estimation of System Damping Parameters using Analytic Wavelet Transforms", IEEE Trans. Power Delivery, vol. 24, No. 3, pp. 1302-1309, July 2009

[3] D. Trudnowski, "Estimating Electromechanical Mode Shape From Synchrophasor measurements", IEEE Trans. Power Syst., vol.23, No.3, pp.1188-1195, Aug. 2008

[4] Roland E. Best. Phase-Locked Loops Design, Simulation and Applications. McGraw-Hill, New York, NY, fifth edition, 2003.

[5] William F. Egan. Phase-Lock Basics. Wiley-Interscience, NewYork, NY, first edition, 1998.

[6] Floyd M. Gardner. Phaselock Techniques. Wiley-Interscience, Hoboken, NJ, third edition, 2005.

[7] Venceslav F. Kroupa. Phase Lock Loops and Frequency Synthesis. John Wiley Sons, Ltd, West Sussex, England, first edition, 2003

[8] H. Meyr, G. Ascheid. Synchronization in Digital Communications Volume I: Phase-, Frequency-Locked Loops, and Amplitude Control. Wiley-Interscience, New York, NY, first edition, 1990.

[9] M. Karimi-Ghartemani, M.R. Iravani, "A nonlinear adaptive filter for online signal analysis in power systems: applications", IEEE Trans. Power Delivery, vol. 17, No. 2, pp.617-622, Apr. 2002

[10] J.R. de Carvalho, C.A. Duque, et al, "A PLL-Based Multirate Structure for Time-Varying Power Systems Harmonic/Interharmonic Estimation", IEEE Trans. Power Delivery, vol. 24, No. 4, pp. 1789-1800, Oct. 2009

[11] M. Ohrstrom, L. Soder, "Fast Protection of Strong Power Systems with Fault Current Limiters and PLL-Aided Fault Detection", IEEE Trans. Power Delivery, vol. 26, No. 3, pp. 1538-1544, July 2011

[12] K. Sun, K. Hur, P. Zhang, "A New Unified Scheme for Controlled Power System Separation Using Synchronized Phasor Measurements", IEEE Trans. Power Syst., vol. 26, No. 3, pp. 1544-1554, Aug. 2011

[13] K. Sun, X. Luo, J. Wong, "Early Warning of Wide-Area Angular Stability Problems Using Synchrophasors", IEEE PES General Meeting, 23-26 July 2012, San Diego, CA

[14] P.D. Welch, "The Use of Fast Fourier Transform for the Estimation of Power Spectra: A Method Based on Time Averaging Over Short, Modified Periodograms", IEEE Trans. Audio Electroacoustics, vol.15, No. 2, pp.70-73, June 1967

[15] FNET, http://fnetpublic.utk.edu/index.html

VII. Biographies

Kai Sun (M'06) received the B.S. degree in automation and the Ph.D. degree in control science and engineering from Tsinghua University, Beijing in 1999 and 2004, respectively. He is currently an assistant professor with the department of electrical engineering and computer science in the University of Tennessee, Knoxville. He was a project manager in grid operations and planning with the Electric Power Research Institute (EPRI), Palo Alto, CA from 2007 to 2012.

Qiang Zhou received his B.S. in Automation and Applied Mathematics from Shanghai JiaoTong University in 1995, a M.S. in Computer Science from Fudan University, Peoples Republic of China, 1998, and a Ph.D. in Electrical Engineering from Ohio University in 2004. His research interests include digital signal and image processing, computer vision, and adaptive communication systems.

Yilu Liu (S'88–M'89–SM'99–F'04) is currently the Governor's Chair at the University of Tennessee, Knoxville and Oak Ridge National Laboratory. Prior to joining UTK/ORNL, she was a Professor at Virginia Tech. Dr. Liu received her MS and Ph.D. degrees from the Ohio State University, Columbus, in 1986 and 1989. She received the BS degree from Xian Jiaotong University. She led the effort to create the North America power grid monitoring network (FNET) at Virginia Tech, which is now operated at UTK and ORNL as GridEye(fnetpublic.utk.edu). Her current research interests include power system wide-area monitoring and control, large interconnection level dynamic simulations, electromagnetic transient analysis, and power transformer modeling and diagnosis.